

Assembly of New Individual Excitatory Synapses: Time Course and Temporal Order of Synaptic Molecule Recruitment

Hagit Vardinon Friedman,* Tal Bresler,*
Craig C. Garner,[†] and Noam E. Ziv*[‡]

*Rappaport Institute and
Department of Anatomy and Cell Biology
Bruce Rappaport Faculty of Medicine
Technion, Haifa 31096
Israel

[†]Department of Neurobiology
The University of Alabama
Birmingham, Alabama 35294

Summary

Time-lapse microscopy, retrospective immunohistochemistry, and cultured hippocampal neurons were used to determine the time frame of individual glutamatergic synapse assembly and the temporal order in which specific molecules accumulate at new synaptic junctions. New presynaptic boutons capable of activity-evoked vesicle recycling were observed to form within 30 min of initial axodendritic contact. Clusters of the presynaptic active zone protein Bassoon were present in all new boutons. Conversely, clusters of the postsynaptic molecule SAP90/PSD-95 and glutamate receptors were found on average only ~45 min after such boutons were first detected. AMPA- and NMDA-type glutamate receptors displayed similar clustering kinetics. These findings suggest that glutamatergic synapse assembly can occur within 1–2 hr after initial contact and that presynaptic differentiation may precede postsynaptic differentiation.

Introduction

The formation of synaptic junctions is a fundamental process during the development and maturation of the mammalian central nervous system (CNS). Until quite recently, much of our understanding of how CNS synapses are formed has come from studies of synaptogenesis at the neuromuscular junction (NMJ) (Hall and Sanes, 1993). Here, axonal growth cones making contact with myotubes are thought to trigger a series of events that lead to the differentiation of both the presynaptic bouton and the postsynaptic reception apparatus. Presynaptically, this includes the clustering of synaptic vesicles (SVs) and the formation of a specialized presynaptic cytoskeletal matrix at the active zone, a site where neurotransmitter release is thought to occur. Similarly, differentiation of the postsynaptic reception apparatus is thought to involve the assembly of a specialized cytoskeletal matrix that serves to localize and cluster neurotransmitter receptors, as well as signaling molecules. Factors released primarily from the newly forming nerve terminals, such as agrin, and neurotransmitter,

are thought to promote the differentiation of the postsynaptic junction (reviewed by Sanes and Scheller, 1997; Hoch, 1999).

While synaptogenesis at CNS synapses could occur in a manner similar to that occurring at the NMJ, this is not at all clear (see, for example, Uchida et al., 1996, and references therein). At present, little is known about the time frame or molecular sequence of events or other factors that direct the assembly of CNS synapses. This is exacerbated by the fact that few instructional proteins identified at the NMJ are also found at CNS synapses or are even required for their formation (Serpinskaya et al., 1999).

The identification and characterization of numerous components of CNS synapses have begun to change this situation (reviewed by Kim and Huganir, 1999; Sheng and Pak, 1999; Garner et al., 2000a, 2000b). Most studies addressing CNS synaptogenesis and the roles of different molecules in this process have followed the temporal expression and distribution patterns of these synaptic proteins in primary cultures of differentiating neurons (Fletcher et al., 1991, 1994; Craig et al., 1993, 1994; Basarsky et al., 1994; O'Brien et al., 1997, 1998, 1999; Rao and Craig, 1997; Rao et al., 1998; Naisbitt et al., 1999; Passafaro et al., 1999; Zhai et al., 2000; see also Verderio et al., 1999). This has led to the conclusion that synaptogenesis at CNS synapses occurs over an extended period of time (days to weeks) (Rao et al., 1998; Lee and Sheng, 2000). In contrast, the use of novel imaging approaches (Cooper and Smith, 1992; Matteoli et al., 1992; Kraszewski et al., 1995; Dailey and Smith, 1996; Ziv and Smith, 1996; Baranes et al., 1998; Engert and Bonhoeffer, 1999; Horch et al., 1999; Maletic-Savatic et al., 1999; Okabe et al., 1999; Toni et al., 1999; Ahmari et al., 2000; Jontes et al., 2000), as well as studies regarding relationships between synaptic activity and the recruitment of postsynaptic α -amino-3-hydroxy-5-methyl-4-isoxazole propionate- (AMPA-) and N-methyl-D-aspartate- (NMDA-) type glutamate receptors (for example, Liao et al., 1999; Shi et al., 1999), indicate that the formation or maturation of CNS synapses is much more dynamic and may occur within a few hours.

What has been lacking in most of these studies is an approach that allows the assembly of new synapses to be followed and distinguished from the numerous synapses already present on any given neuron. This would allow many of the fundamental questions regarding the temporal formation of functional synapses to be addressed, including the following. (1) What is the time course of the formation of functional synapses? (2) Is the active zone assembled sequentially or in parallel to the postsynaptic density (PSD)? (3) Which synaptic proteins are present early during the assembly process of individual synapses and thus are likely to play instructive roles? (4) Which synaptic molecules accumulate later, after most of the synaptic scaffold has been laid down, and thus probably have little to do with the primary processes of synaptic assembly? And finally, (5) do certain types of postsynaptic receptors accumulate at new synapses before other types do?

[‡]To whom correspondence should be addressed (e-mail: noamz@netvision.net.il).

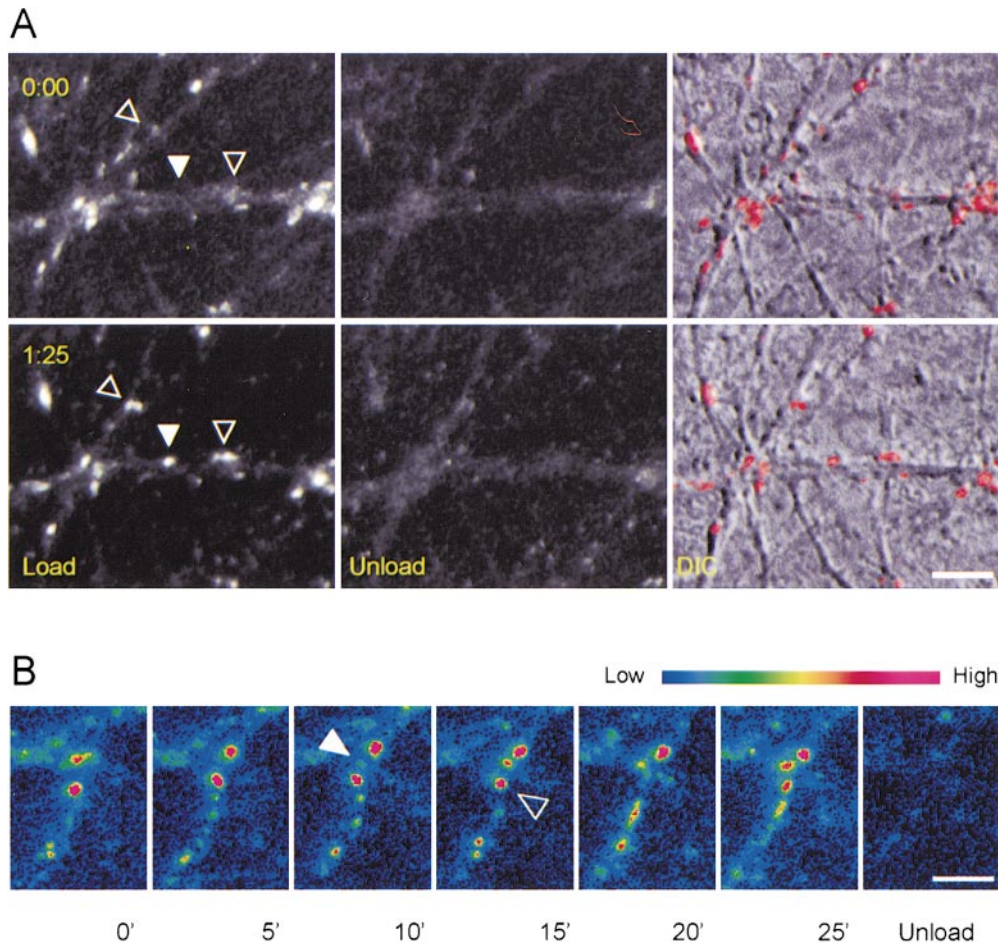


Figure 1. Appearance of Apparently New Presynaptic Bouton Detected by Labeling with FM 4-64

(A) Recurrent labeling of SVs with FM 4-64 reveals apparently new presynaptic boutons. The preparation showed here was labeled with FM 4-64 as described in text (top panels) and then again after 85 min (bottom panels). Fluorescent puncta, most likely presynaptic boutons, are clearly visible (left-hand panels). A 2 min train of action potentials leads to the destaining of most puncta, leaving behind only faint background fluorescence (middle panels), suggesting that the fluorescently labeled puncta in the left-hand panels were functional presynaptic boutons capable of activity-invoked exocytosis. Spatial relationships with dendrites are shown by overlaying fluorescence data (red) over DIC images of the same regions (right-hand panels). Note the appearance of three bright puncta after the second labeling episode (arrowheads in left-hand panels). However, as faint punctate fluorescence was detectable at the locations of two of these puncta after the first labeling episode (open arrowheads), they were excluded from analysis. No punctate fluorescence is observed at the position of a third fluorescent spot (closed arrowheads), suggesting that a new bouton may have formed at this location.

(B) Time-lapse of SVs labeled with FM 4-64 at 5 min intervals. Note the rapid appearance of a new cluster of SVs (closed arrowhead, $t = 10'$). The intensity of puncta in the field of view changes from one image to another, suggesting that labeled vesicles are being mobilized among nearby persistent sites. For example, note the disappearance of the large spot at $t = 15'$ (open arrowhead) and its reappearance 10 min later. Fluorescence intensities (arbitrary units) are coded using a pseudocolor look-up table shown above the images.

Scale bars, 5 μm .

In this study, we describe experiments designed to determine the time frame of individual glutamatergic synapse assembly and the temporal order in which specific pre- and postsynaptic molecules are recruited to new synaptic junctions. This has been accomplished by establishing a novel approach that allows the identification of newly forming synapses in these cultures, complemented with retrospective immunohistochemical methods used to measure the accumulation kinetics of specific synaptic proteins at such new synapses. Our studies reveal that individual glutamatergic synapses between cultured hippocampal neurons can form over a period of 1–2 hr and that the formation of a functional presynaptic bouton often precedes the differentiation of the postsynaptic reception apparatus.

Results

Recurrent Labeling of Synaptic Vesicles with FM 4-64 Reveals the Appearance of Apparently New Presynaptic Boutons

The initial objective of this study was to establish a method that would allow us to determine when and where new synapses were being formed between hippocampal neurons in primary culture. These experiments were performed in neurons maintained 11–14 days in vitro (DIV), the peak period of synaptogenesis in our culture system (Ziv and Smith, 1996). To determine when and where new synapses were being formed, the fluorescent endocytotic dye FM 4-64 was employed due to its ability to label SVs in living neurons in response to

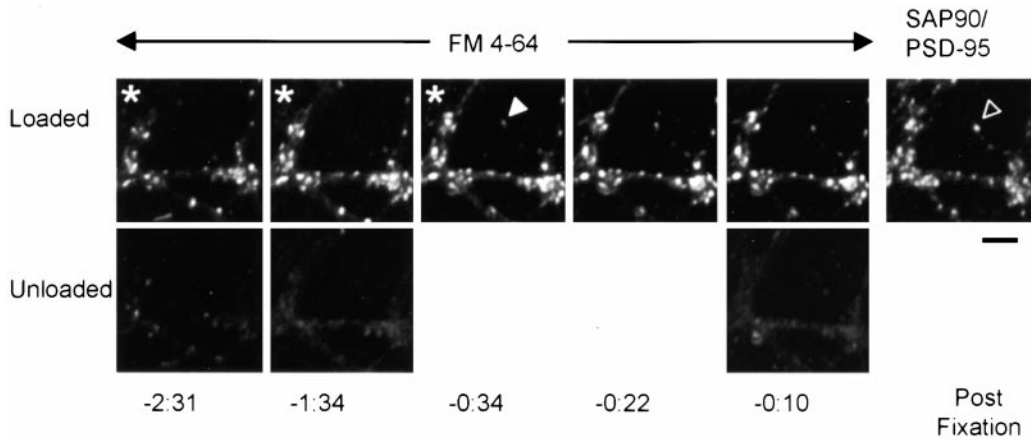


Figure 2. Clustering of the PSD Protein SAP90/PSD-95 at New Synaptic Sites

Recurrent labeling with FM 4-64 and time-lapse imaging of labeled SVs were used to detect the appearance of an apparently new presynaptic bouton (arrowhead, $t = -0:34$). Note that this new cluster was not observed prior to this time point; however, once it appeared, it remained at the same location until the end of the experiment. Retrospective immunohistochemistry of the same region revealed that the apparently new bouton was associated with a discrete cluster of SAP90/PSD-95. Images collected immediately after a labeling episode of SVs with FM 4-64 are marked with asterisks. Time is given as hours and minutes relative to the moment of fixation and refers to 5 images in the top panels. Images obtained after destaining stimulation trains (bottom panels) were collected ~ 5 min after those above them. Scale bar, 5 μm .

presynaptic activation (Henkel and Betz, 1995; Ziv and Smith, 1996; see also Ryan et al., 1993, 1996; Ryan and Smith, 1995; Cochilla et al., 1999).

Figure 1A shows an example of a population of presynaptic boutons labeled with FM 4-64. These boutons were labeled by stimulating the neurons to fire action potentials for 30 s in the presence of 15 μM FM 4-64. All stimulation was performed by passing 1 ms current pulses at 10 Hz through field stimulation electrodes embedded in the chamber; 30 s after the end of the stimulation episode, the dye was washed out for 15 min, and images were collected. To determine which fluorescent puncta represent activity-induced exocytosis/endocytosis of SVs, neurons were then stimulated to fire a second train of action potentials for 120 s at 10 Hz to induce exocytosis of the labeled SVs. Fluorescent puncta that appeared after the labeling (load) procedure and disappeared after the destaining stimulation episode (unload) were considered to represent functional presynaptic boutons (Figure 1A). The ionotropic glutamate receptor antagonists 6,7-dinitroquinoxaline-2,3-dione (DNQX, 10 μM) and 2-amino-5-phosphonopentanoic acid (AP-5, 50 μM) were included in the perfusion solution for the duration of all experiments, in order to block stimulation-induced network reverberations. This assured that each stimulus caused at most a single action potential. Furthermore, it reduced the dye loss from loaded boutons otherwise caused by spontaneous network activity.

To detect the appearance of newly formed presynaptic boutons, this procedure was repeated at various time intervals. When recurrent labeling of SVs was performed, new fluorescent puncta, apparently representing new presynaptic boutons, were observed at previously unlabeled locations. Such fluorescent puncta were scored as new boutons only when no labeling was detected after the first labeling episode (Figure 1A). Typically, one to two new fluorescent puncta were detected per field of view per hour, which represented $<1\%$ of the number of preexisting boutons in the field. To increase the number of events detected in a single experiment, we collected data from up to 12 (but typically 4–5) fields of

view (sites) in each experiment using the automated XYZ stage on our confocal laser scanning microscope (CLSM). Potential errors caused by focal plane drift (for example, boutons moving in and out of the focal plane) were minimized by using the automatic focusing feature of our CLSM and collecting four sections at 1 μm intervals at each site (see Experimental Procedures). As the preparations are typically only 2–3 μm thick, we are confident that the appearance of these apparently new boutons is not an artifact of focus errors.

Although recurrent SV labeling enabled us to record the appearance of apparently new presynaptic boutons, the time resolution of this method was rather low (up to two samples per hour). This limitation was overcome in part by following the distribution of the labeled SVs by time-lapse microscopy before unloading the dye. When the labeled SVs were examined at 5 min intervals, most preexisting synaptic boutons appeared to be rather stable. Occasionally, however, we observed rapid changes in the distributions of labeled SVs among nearby boutons, suggesting that SVs were being mobilized along axonal segments between adjacent en passant boutons. Furthermore, we recorded numerous instances in which SVs were mobilized to new sites at which no SVs were previously observed, suggesting that they were being recruited to new synaptic sites (Figure 1B). Moreover, nearly all labeled SVs, including those that had accumulated at new sites, disappeared following a 2 min destaining stimulation episode (1200 action potentials delivered at 10 Hz), suggesting that new and functional presynaptic boutons had formed at these sites.

Previous studies have documented the existence of nonsynaptic, motile SV clusters that often display activity-dependent exocytosis or endocytosis (Matteoli et al., 1992; Kraszewski et al., 1995; Dai and Peng, 1996). We too have observed such motile clusters. However, in agreement with a previous report (Kraszewski et al., 1995), they appeared to be smaller (composed of less labeled vesicles) than were the apparently new presynaptic boutons. Furthermore, the formation of most new SV cluster sites did not seem to result simply from the

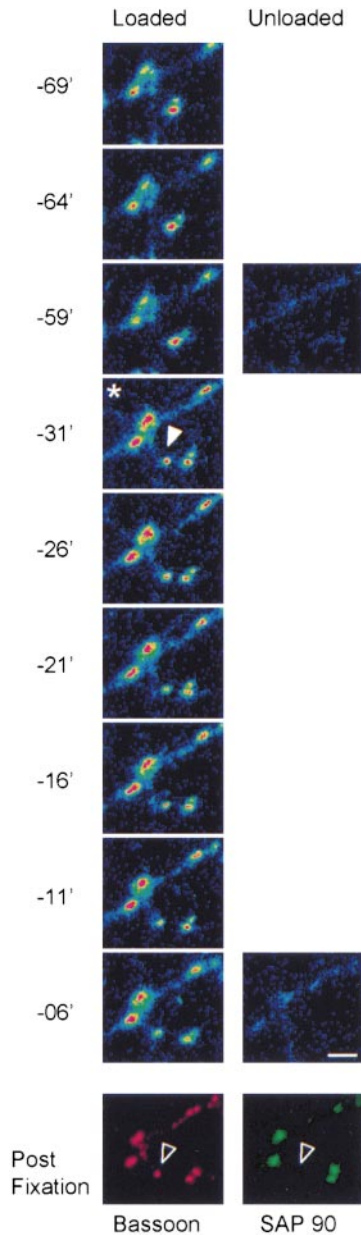


Figure 3. Clustering of the Presynaptic Active Zone Protein Bassoon at New Synaptic Sites

Recurrent labeling with FM 4-64 intermixed with time-lapse imaging of the labeled SVs revealed the appearance of an apparently new presynaptic bouton (closed arrowhead, $t = -31'$). Retrospective immunohistochemistry of the same region revealed that this apparently new bouton was associated with a discrete cluster of Bassoon but not with SAP90/PSD-95 (open arrowheads, bottom panels). Fluorescence intensity in FM 4-64 time series is coded using a pseudocolor look-up table, as in Figure 1B. First image collected after the second labeling episode is marked with an asterisk. Time is given as minutes relative to the moment of fixation and refers to images in the left-hand panels. Images obtained after destaining stimulation trains (right panels) were collected ~ 5 min after those to their left. Scale bar, 3 μm .

movement or aggregation of discrete SV clusters. Rather, they seemed to involve en masse SV mobilization from nearby loci, as suggested by the occasional

appearance of elongated "bands" of fluorescently labeled SVs between adjacent, relatively persistent loci (for example, see Figure 1B, time = 00:20').

The greater temporal resolution offered by time-lapse recordings of labeled vesicles and the additional data they provided regarding the persistence and origin of new SV clustering sites prompted us to include such time-lapse imaging of SVs in our experimental protocol. Thus, in all experiments described below, the following protocol was used to detect the appearance of new presynaptic boutons. SVs were labeled periodically with FM 4-64. Then, labeled SVs were followed for 10–40 min at 5 min intervals. Finally, a stimulation train was used to unload the dye. This routine was repeated two to three times in each experiment.

The additional data provided by these time-lapse series allowed us to further refine our criteria for scoring new FM 4-64 puncta as new presynaptic boutons. These criteria are summarized as follows: no punctate FM 4-64 labeling was detected at the putative site immediately after the first labeling episode; once formed, the SV cluster persisted at approximately the same location until the end of the time-lapse session; the cluster did not originate from a large cluster splitting into smaller ones; its size was similar to that of preexisting, persistent SV clusters; and it had to release the dye in response to the destaining stimulation train.

Many of the new SV clusters we detected conformed with these criteria. About 20% were observed to form during time-lapse recordings of labeled SVs (as in Figure 1B), while the remaining 80% were detected immediately after recurrent labeling episodes (as in Figure 1A). These findings suggest that recurrent FM 4-64 labeling of SVs intermixed with time-lapse recordings of these SVs can be used to detect the appearance of new functional presynaptic boutons and to determine when such boutons first display a capacity for activity-induced SV recycling. The time at which this capacity was first manifested was used thereafter as a reference time to which all other events were related.

Accumulation Dynamics of the Cytomatrix Molecules Bassoon and SAP90/PSD-95 at New Synaptic Sites

The assembly of the presynaptic active zone and the postsynaptic reception apparatus has been hypothesized to be orchestrated by specific molecules (Kim and Haganir, 1999; Garner et al., 2000a, 2000b). The presynaptic cytomatrix protein Bassoon is a recently identified component of the presynaptic active zone implicated to play a role in defining neurotransmitter release sites (tom Dieck et al., 1998; Brandstatter et al., 1999; Richter et al., 1999; Winter et al., 1999; Zhai et al., 2000). Conversely, the postsynaptic molecule SAP90/PSD-95 is thought to play important roles in organizing the PSD and in localizing postsynaptic NMDA receptors (Cho et al., 1992; Kistner et al., 1993; Kornau et al., 1995; see also Garner et al., 2000b, and references therein).

A retrospective immunohistochemical analysis of new synaptic boutons was therefore performed to address two questions. First, are the "newly formed synapses" identified by recurrent FM 4-64 labeling associated with clusters of known structural components of synaptic junctions and thus likely to represent "real" synapses? Second, is the temporal order of appearance of these two proteins at nascent synapses consistent with the

roles attributed to them? To this end, the appearance of new presynaptic boutons was recorded as described above, after which the specimens were rapidly fixated and stained with antibodies directed against Bassoon and/or SAP90/PSD-95 (see Experimental Procedures). We then determined for each apparently new bouton if a cluster of Bassoon or SAP90/PSD-95 was present at the same location. These data were then compared with the bouton's "age," defined as the time interval between the moment the bouton was first observed and the time at which the preparation was fixed. (Note that the age assigned to boutons that appeared immediately after a labeling procedure was based on the time at which they were labeled with FM 4-64, not the time they were first imaged. See Experimental Procedures for details.)

Figure 2 shows an example of a new bouton that appeared ~54 min before fixating the preparation. Retrospective analysis revealed that the same bouton was also labeled with antibodies against SAP90/PSD-95. Similarly, Figure 3 shows that a new bouton that appeared ~45 min before fixation was clearly labeled with antibodies against Bassoon but not SAP90/PSD-95. These data strongly support the likelihood that our recurrent labeling approach identifies bona fide synaptic junctions.

To determine the accumulation kinetics of these molecules at nascent synapses, all boutons observed to form in these experiments were categorized according to their "age," and the fraction of boutons in each age group found to be matched with clusters of Bassoon or SAP90/PSD-95 was compared with the fraction of preexisting boutons (>99%) associated with clusters of these molecules (Figures 4A and 4B).

For Bassoon (Figure 4A), we found that 95% of all preexisting boutons detected before fixation by FM 4-64 labeling were matched with a distinct cluster of this molecule (2269 boutons, 20 sites, 5 experiments). A similar fractional match was observed for "new" boutons from all age groups, including the very earliest age group. These findings suggest that Bassoon clusters at presynaptic sites before or concomitantly with the acquisition of a capacity for activity-induced recycling of SVs, which is consistent with Bassoon playing an instructional role in the assembly of new presynaptic active zones.

In the case of SAP90/PSD-95, the fractional match of preexisting boutons was ~58% (3392 boutons, 24 sites, 6 experiments). However, in contrast to what we found for Bassoon, the fraction of boutons matched with discrete clusters of SAP90/PSD-95 clearly increased with bouton "age," from 29% in the youngest age group (<45 min) to 59% in the oldest (75–120 min). (Figure 5B). This may be interpreted to suggest that SAP90/PSD-95 is recruited to synaptic junctions somewhat later than Bassoon is (but see Discussion).

Accumulation Dynamics of Postsynaptic Glutamate Receptors at New Synaptic Sites

The capacity of a glutamatergic synapse to convey signals across the synaptic gap depends on the presence of glutamate receptors in the postsynaptic membrane. To determine when ionotropic glutamate receptors appear at nascent synapses, we recorded the appearance of new presynaptic boutons using FM 4-64 as described above. Cultures were then fixed and double stained with antibodies directed against the GluR1 and NR1 subunits

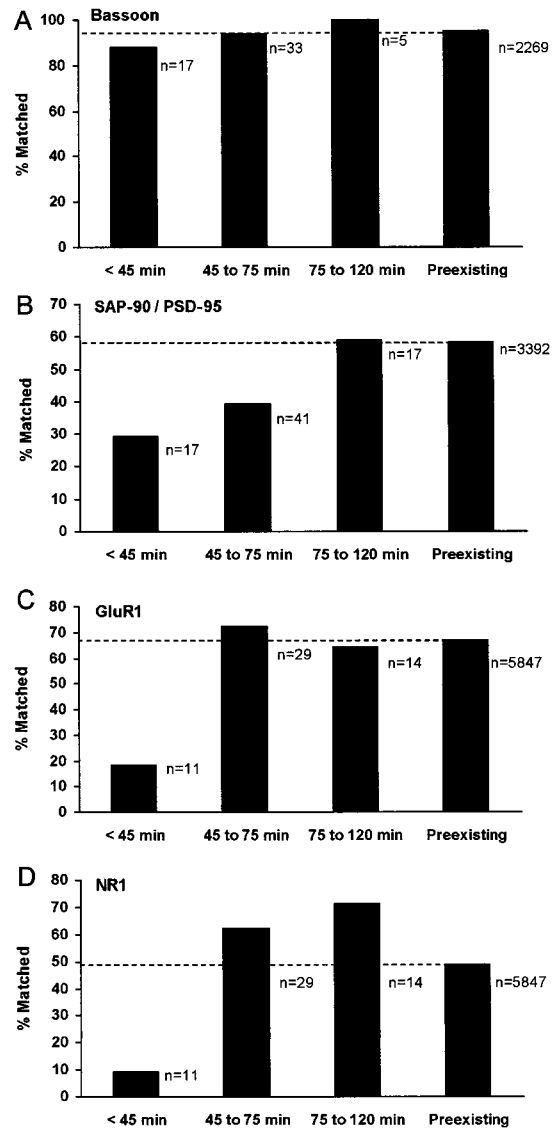


Figure 4. Accumulation Kinetics of Four Synaptic Proteins at Nascent Synapses

(A) Bassoon.

(B) SAP90/PSD-95.

(C) GluR1.

(D) NR1. New boutons detected by FM 4-64 labeling were grouped according to their "age," defined as the time interval between the moment the bouton was first observed and the time at which the preparation was fixed (see text). Each bar represents the fraction of new presynaptic boutons in each age group that was found to be tightly associated with a discrete cluster of one of four specific molecules, as determined in retrospect by immunohistochemistry. Numbers beside each bar indicate the total number of boutons within each age group. The bars labeled "Preexisting" reflect the fractions of all boutons (old and new) that were tightly associated with clusters of such molecules. As these groups are composed mainly of boutons observed to be present from the very beginning of the experiment (>99%), they represent almost entirely the populations of preexisting boutons. Note the differences in the accumulation kinetics of the presynaptic molecule Bassoon as compared with those of the postsynaptic molecules SAP90/PSD-95, GluR1, and NR1.

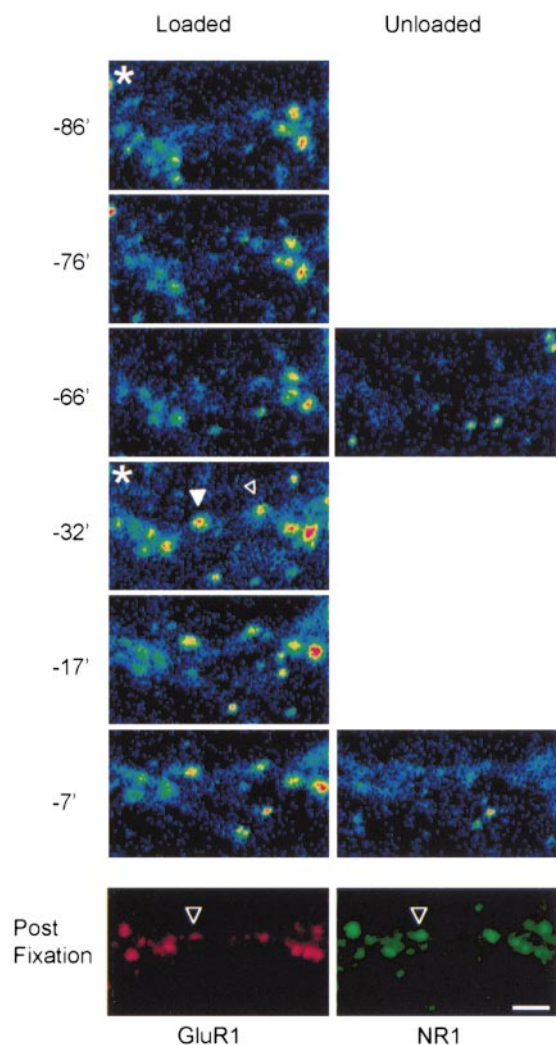


Figure 5. Clustering of Glutamate Receptors at New Synaptic Sites
FM 4-64 fluorescence microscopy revealed the appearance of an apparently new presynaptic bouton after a second labeling episode (closed arrowhead, $t = -32'$). Retrospective immunohistochemistry of the same region revealed that this new bouton was associated with discrete clusters of GluR1 and NR1 (open arrowheads, bottom panels). A second SV cluster that seemed to appear after the second round of FM 4-64 labeling (small open arrowhead, $t = -32'$) was not included in the analysis since it was detected after the first labeling episode. Fluorescence intensity in FM 4-64 time series is coded using a pseudocolor look-up table, as in Figure 1B. First images collected after a labeling episode are marked with asterisks. Time is given in minutes relative to the moment of fixation and refers to images in the left-hand panels. Images obtained after the destaining stimulation trains (right panels) were collected ~ 5 min after those to their left. Scale bar, $3 \mu\text{m}$.

of the AMPA- and NMDA-type ionotropic glutamate receptors, respectively. Each apparently new bouton was then examined to determine if it was associated with a discrete cluster of GluR1, NR1, or both. An example of a new bouton that labeled with both GluR1 and NR1 antibodies is shown in Figure 5. This particular bouton appeared after a second labeling round performed 52 min before fixation and persisted until the end of the experiment.

The results of these experiments are summarized in Figures 4C and 4D. This analysis reveals that for preexisting boutons, 67% were found to be associated with clusters of GluR1, and 49% were associated with clusters of NR1 (5847 boutons, 43 sites, 9 experiments). In contrast, for boutons detected within 45 min of fixation, only 18% and 9% were associated with GluR1 or NR1 clusters, respectively. The fractional match of older boutons that had appeared during these experiments was similar or slightly greater than that observed in preexisting boutons.

Interestingly, 37% of preexisting boutons were found to be associated with both GluR1 and NR1 clusters, while 30% and 12% contained primarily AMPA or NMDA receptors, respectively. In total, these data indicate that $\sim 79\%$ of synapses detected here were glutamatergic synapses. It follows that 47% of these synapses contained significant numbers of both NMDA- and AMPA-type glutamate receptors, while 38% and 15% contained primarily AMPA or NMDA receptors, respectively. In the population of apparently new synapses, the numbers were similar (60%, both types; 24%, AMPA alone; 16%, NMDA alone, all nascent synapse age groups). However, a somewhat larger proportion of presumably glutamatergic synapses contained both AMPA- and NMDA-type glutamate receptors.

These experiments suggest that the clustering of glutamate receptors of both types lags behind the differentiation of presynaptic specializations by ~ 45 min. No substantial difference was found in the clustering kinetics of GluR1 versus NR1.

Presynaptic Boutons Can Form Rapidly after the Establishment of Axodendritic Contacts

A fundamental issue unresolved by the experiments described above is how soon after the initial contact of axons and dendrites is a capacity for activity-induced recycling of SVs acquired. To obtain an estimate of the time required for a presynaptic bouton to form and display activity-induced SV recycling relative to the time of initial cell-cell contact, the formation of new contacts between axons and dendrites was followed with time-lapse fluorescence microscopy while periodically labeling SVs with FM 4-64 to monitor the appearance of newly forming boutons. As the morphological complexity of the neuronal network in our culture system severely limits the ability to resolve the fine structure of axonal and dendritic processes (Ziv and Smith, 1996), some method for labeling individual axons and dendrites was necessary. To that end, a DNA transfection method was used to express enhanced green fluorescent protein (EGFP) in a small fraction ($<1\%$) of the neurons. Although few axons and dendrites were labeled in this manner, we managed to record the establishment of four axodendritic contacts that seemed to result in the formation of apparently functional presynaptic boutons, as determined by FM 4-64 labeling (Figure 6). Evoked SVs recycling at each of these four sites was observed 26, 24, 24, and 32 min after axodendritic contacts were established. As only a small subset of neurites were labeled with EGFP (and were hence visible), it remains possible that the new boutons had in fact formed between unlabeled adjacent axons and/or dendrites. In one case, however, differential interference contrast (DIC) imaging enabled us to observe all neurites within the vicinity of

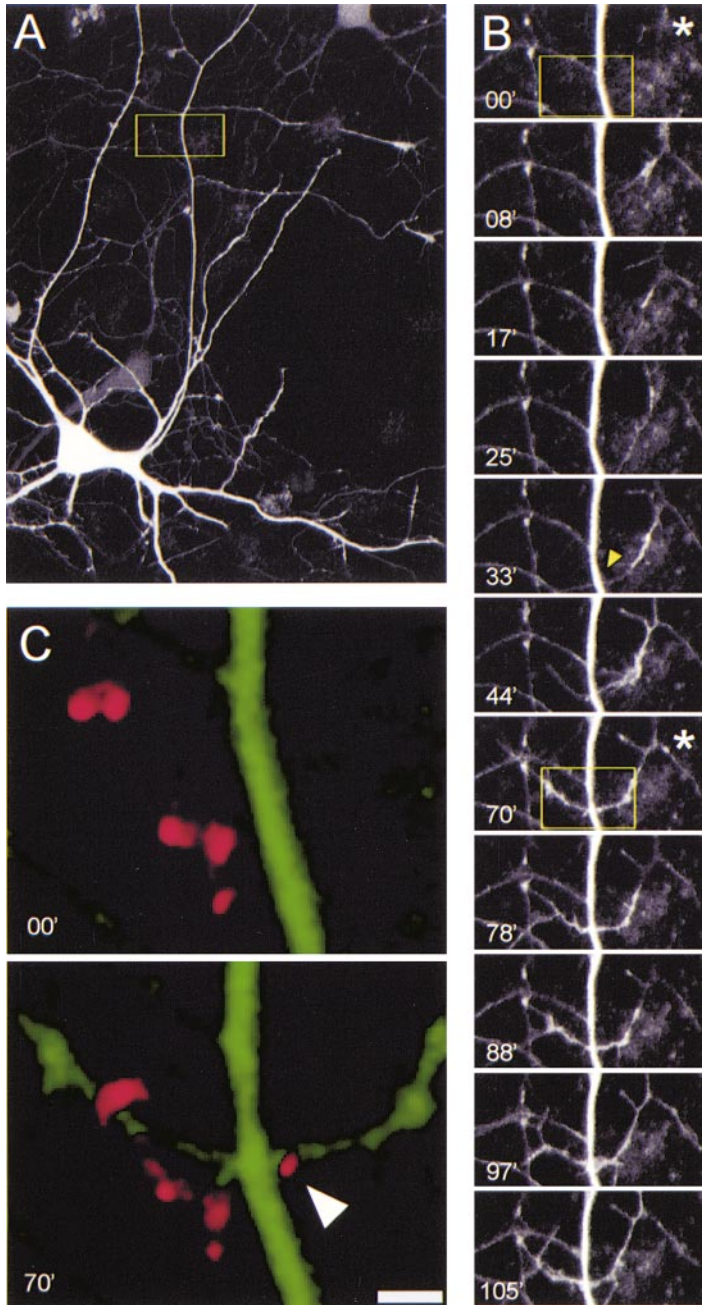


Figure 6. Formation of a Presynaptic Bouton following New Axodendritic Contact

(A) A hippocampal neuron expressing EGFP. (B) Time-lapse sequence showing an axonal growth cone coming out of the top right corner, encountering the dendritic segment seen at the center of the image ($t = 33'$, yellow arrowhead) and crossing over to the left. This is an enlargement of the region enclosed in a yellow rectangle in (A). First images collected after a labeling episode are marked with asterisks.

(C) Recurrent FM 4-64 labeling revealed that a new bouton had appeared at the intersection site of the dendrite and the ingrowing axon (closed arrowhead). Regions shown correspond to respective areas enclosed in yellow rectangles in (B). Scale bar, 2 μm .

the new bouton and to unequivocally determine that it had indeed formed between a single axon and a single dendrite that had just formed a new intersection (data not shown). These observations indicate that functional active zones may form as soon as 25–30 min after initial cell–cell contact.

Interestingly, we also observed contacts that did not lead to the formation of new synaptic boutons. Many of these contacts were transient, but some seemed to persist for the duration of the experiment. These observations may suggest that some presynaptic boutons form over time periods that exceed the duration of these experiments. Alternatively, they may simply suggest that many axodendritic encounters do not result in the formation of new synapses (see Discussion).

Discussion

We have used cultured hippocampal neurons, live imaging, and retrospective immunohistochemical methodologies to determine the time frame for the formation of glutamatergic synapses and examine the temporal order in which specific pre- and postsynaptic molecules cluster at new synapses. Our studies reveal that functional presynaptic boutons can form within 25–30 min of the establishment of an axodendritic contact. In some cases, the formation of such boutons seems to be associated with the recruitment of SVs from nearby pre-existing boutons. Using retrospective immunohistochemistry, we found that such new synaptic boutons practically always contained a cluster of the presynaptic

cytomatrix molecule Bassoon. Conversely, the appearance of the postsynaptic components SAP90/PSD-95, GluR1, and NR1 seemed to lag behind the appearance of the presynaptic boutons by ~ 45 min. Taken together, these findings suggest that new glutamatergic synapses may form over periods of 1–2 hr and that the formation of a functional presynaptic bouton precedes the assembly of the postsynaptic compartment.

Time Frame of Individual Glutamatergic Synapse Assembly

The simplest interpretation of the experiments described here is that glutamatergic synapses can form as fast as 1–2 hr after an axodendritic contact has been established. In arriving at this conclusion, however, we also consider several alternative interpretations.

A key assumption in the design of our experiments was that the appearance of new, activity-induced clusters of FM 4-64-labeled SVs implied that a new bouton had formed at that site. It is possible, however, that such boutons were preexisting boutons that for some reason responded weakly or not at all to stimulation in the initial labeling episodes (and thus did not uptake dye) but did respond later on. At the extreme, such boutons could be viewed as “presynaptically silent” synapses (Ma et al., 1999; see also Kannenberg et al., 1999). While possible, several arguments can be made against this interpretation. First, all experiments were performed in the presence of AP-5 and DNQX, treatments previously shown to abolish completely activation of such “presynaptically silent” boutons (Ma et al., 1999) or to block an increase in their probability of release (Ryan et al., 1996). Second, we discarded boutons for which the slightest labeling in initial labeling episodes was observed; thus, for a preexisting bouton to escape detection, it would have to be almost completely unresponsive to electrical stimulation and display very low rates of spontaneous vesicle recycling. Third, we observed strong relationships between the age of such boutons and the degree to which they were matched with three postsynaptic components (SAP90/PSD-95, GluR1, and NR1). Such relationships would hardly be expected for preexisting synapses. Fourth, the number of apparently new boutons detected per field of view per hour is in agreement with the rate of synapse addition in cultures 9–14 DIV. For example, we typically observe about 100–250 preexisting boutons per field of view. Assuming a constant rate of synapse addition during a 6 day period (e.g., 9–14 days), 1–2 boutons would be expected to appear per field of view per hour, on average.

Another concern is that not all new boutons were followed for the same duration. In fact, the “youngest” boutons, those that appeared immediately before fixation, were only observed at two time points (including the observation made after dye unloading). It follows that some “young” boutons could have been mobile vesicle clusters rather than persistent boutons. Such mobile clusters could have escaped recognition, as this was based in part on comparisons of their positions in series of sequential images. While we cannot completely rule out this possibility, it is worth noting that, apart from four puncta, all FM 4-64-labeled puncta scored as new boutons were imaged at least twice before destaining. Moreover, all clusters scored as new boutons appeared to be rather large, comparable in size (or in labeled vesicle number) to preexisting boutons. In contrast,

most mobile SV clusters appeared to be much smaller (see also Kraszewski et al., 1995). Finally, nearly all FM 4-64 puncta scored as new boutons were associated with a cluster of Bassoon, a presynaptic active zone molecule that is not a SV protein (tom Dieck et al., 1998). Thus, it is quite unlikely that the late appearing SV clusters were mobile clusters of SVs moving along axons.

It is also important to note that the “age” assigned to apparently new boutons is inherently inaccurate to some degree. This is due to the fact that many new boutons were detected following a second or third round of FM 4-64 labeling, and the “birth date” assigned to such boutons was the time at which the labeling procedure was performed. It is almost certain, however, that many of these boutons had become functional before this labeling episode (but after the prior labeling episode), and, thus, the age assigned to them underestimated their true age. In addition, a small fraction of boutons may have formed slightly after the labeling episode, as shown in Figure 1B. We thus grouped apparently new presynaptic boutons into rather broad age categories that matched the limited temporal resolution of our dating method.

Taken together, these data reveal that new glutamatergic synapses may form between cultured hippocampal neurons over periods of 1–2 hr. This time range agrees well with recent studies showing that new spines can form in rat hippocampal organotypic slice cultures within 1 hr or less of an episode of high-frequency stimulation (Engert and Bonhoeffer, 1999; Maletic-Savatic et al., 1999; Toni et al., 1999) and with earlier studies on spontaneous spine formation (Dailey and Smith, 1996; Ziv and Smith, 1996). Furthermore, a very recent report of Ahmari et al. (2000) vividly demonstrated that vesicular transport packets containing a GFP-tagged SV protein (VAMP) can accumulate rapidly at new axodendritic contacts sites, and within 1 hr, this site can acquire a capacity for activity-induced vesicle recycling. Yet, it must be noted that as with all of the studies listed above, we did not determine the capacity of new synaptic junctions for synaptic transmission. It is conceivable, for example, that the immunolabeled glutamate receptors found at new synaptic junctions were in fact cytoplasmic, rather than receptors located in the postsynaptic membrane, as we permeabilized the cells before immunostaining them. While this specific possibility does not seem likely (as reported by Mammen et al., 1997; O'Brien et al., 1997, 1998; Liao et al., 1999), the mere presence of these receptors does not necessarily indicate that the postsynaptic receptive apparatus was fully functional. Still, our study has gone further toward establishing the functionality of such nascent synapses: the demonstrated capacity for evoked neurotransmitter release at these new presynaptic sites, combined with the documented presence of glutamate receptors at the same sites, makes the possibility that these nascent synapses had some capacity for synaptic transmission quite likely.

The Temporal Order of Synaptic Assembly

Assuming that an imaginary time line can be used to describe the assembly process of individual glutamatergic synapses, our experiments suggest that synaptogenesis typically proceeds according to a temporal sequence summarized schematically in Figure 7. The steps involve (1) formation of an axodendritic contact,

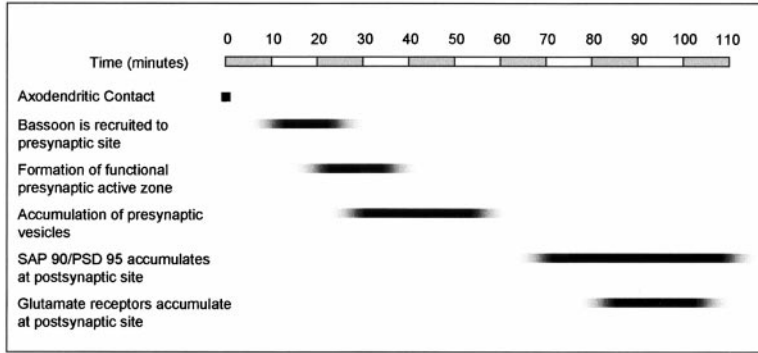


Figure 7. Proposed Time line of Glutamatergic Synapse Assembly

The putative timing of key events during the assembly of individual glutamatergic synapses as deduced from the findings described in this study. Note that this time line probably represents typical time frames for these events, but the actual timing may vary significantly between individual synapses, as suggested by the data in Figure 4 and discussed in the text.

(2) recruitment of presynaptic cytomatrix proteins, such as Bassoon, (3) formation of a functional active zone that possesses a capacity for activity-induced exocytosis and endocytosis, (4) recruitment of SVs to the new active zone, and (5) clustering of SAP90/PSD-95 and postsynaptic glutamate receptors at the postsynaptic membrane.

This proposed temporal sequence is based primarily on our observation that postsynaptic molecule recruitment appears to lag behind presynaptic differentiation. It must be noted, however, that the analysis method applied in this study is asymmetrical, i.e., we first located differentiated presynaptic structures and then examined the degree of their postsynaptic differentiation. It is imaginable that if the appearance of new synapses was detected by locating differentiated postsynaptic structures, we would also find synapses whose presynaptic differentiation occurred later on. Thus, until such complementary studies are performed, one should keep in mind that the temporal order proposed above is one possible interpretation but not necessarily the only one. Still, it should be noted that if pre- and postsynaptic differentiation occurred completely in parallel, 50% of new boutons on average would be associated with differentiated postsynaptic structures at the time of their appearance. This does not seem to be the case for glutamate receptors (Figure 4), although this seems possible for SAP90/PSD-95, which may suggest that this molecule clusters at nascent synapses before glutamate receptors do. This temporal order would agree well with the role proposed for SAP90/PSD-95 in clustering NMDA-type glutamate receptors (reviewed by Kim and Huganir, 1999; Garner et al., 2000b; but see Migaud et al., 1998; Passafaro et al., 1999).

If functional presynaptic boutons form before glutamate receptors cluster at the postsynaptic membrane, it could suggest that factors released by the presynaptic bouton induce the assembly of the postsynaptic compartment. At present, it appears unlikely that glutamate plays this role, since postsynaptic differentiation occurred in our experiments in the presence of ionotropic glutamate receptor antagonists, which is in agreement with previous reports (Craig et al., 1994; Kossel et al., 1997; Verhage et al., 2000). This suggests that other factors may be responsible for coordinating the differentiation of the pre- and postsynaptic compartments, like agrin does at the NMJ (Hoch, 1999). Some potential candidates include molecules such as Narp (O'Brien et al., 1999) or cadherins (Shapiro and Colman, 1999).

The presence of the presynaptic protein Bassoon in practically all new synaptic boutons is particularly intriguing. This protein is a member of a recently discovered

family of large presynaptic proteins found in close proximity to presynaptic active zones (Fenster et al., 2000; Garner et al., 2000a) and is thought to play a role in organizing sites of regulated neurotransmitter release (tom Dieck et al., 1998; Zhai et al., 2000). Interestingly, we have recently found that Bassoon is transported to nascent synapses on a transport vesicle that contains additional active zone molecules (C. C. Garner et al., submitted). This raises the intriguing possibility that such vesicles may constitute "preassembled" active zones, providing a mechanism for the rapid formation of new active zones (see also Ahmari et al., 2000).

Electron microscopy of newly formed presynaptic sites reveals a surprising paucity of "classical" SVs (Ahmari et al., 2000). We thus suggest that the accumulation of SVs at nascent presynaptic sites occurs after such sites are formed (Figure 7). While it is possible that new SVs form in situ, observations such as those of Figure 1B may suggest that SVs are also recruited from nearby boutons. These findings may be interpreted to suggest that SVs constitute a limiting resource during peak periods of synaptogenesis.

Several studies have suggested that AMPA-type receptor recruitment to new glutamatergic synapses is preceded by NMDA-type receptor clustering and that the activation of NMDA receptors may actually induce the insertion of non-NMDA glutamate receptors at such synapses (reviewed by Feldman and Knudsen, 1998; see also Liao et al., 1999; Petralia et al., 1999). As all experiments described here were performed in the presence of glutamate channel antagonists, the roles of synaptic activation in receptor clustering could not be evaluated. In the presence of these antagonists, the accumulation kinetics of NR1 and GluR1 at nascent synapses appeared similar (Figure 4). In addition, we found a significant fraction of apparently new boutons (24%) that were associated with a cluster of GluR1 receptor subunits but not with a cluster of NR1 subunits. Yet, we did find a greater fraction of synapses matched with clustered NR1 in the population of new synapses as compared with that in preexisting ones (Figure 4D). No such trend was observed for AMPA-type receptors (Figure 4C). This may suggest that as synapses mature, they lose some of their NMDA-type glutamate receptors. Still, our findings indicate that AMPA-type glutamate receptors may cluster at new synaptic sites even in the presence of NMDA- (and AMPA-) type glutamate receptor antagonists, questioning the necessity of NMDA-type glutamate receptor activation for the initial recruitment of AMPA-type glutamate receptors to new synapses (see also Rao and Craig, 1997).

Conclusion

Our findings suggest that individual glutamatergic synapses may form within 1–2 hr of the establishment of a new axodendritic contact. Although this is significantly less than the time required for the formation of a fully formed neuromuscular synapse (Buchanan et al., 1989), it is not surprising, given the structural complexity of the NMJ. Still, the time required for the formation of a central glutamatergic synapse is not negligible, and if such processes are considered as mechanisms of memory consolidation, this time frame should be brought into account.

It is worth reiterating that many axodendritic contacts we observed to form did not result in the formation of new synaptic boutons within the time frame of the time-lapse sessions. While this may suggest that most contacts are nonsynaptogenic in nature, it is also possible that new synapses would have formed eventually at these sites, albeit over longer time periods. This raises an interesting question as to the necessity of a new contact for the formation of a new synapse, and one wonders if new synapses may form at preexisting axodendritic contact sites (but see Cooper and Smith, 1992). This is only one example of several surprisingly simple but as yet unanswered questions regarding synapse formation in the CNS. Further studies applying similar strategies or employing more specific molecular markers, such as fluorescently tagged synaptic proteins should clarify such issues and will undoubtedly improve our understanding of synaptic assembly and the roles of specific molecules in this process.

Experimental Procedures

Cell Culture

Hippocampal cell cultures were prepared as described previously (Ryan et al., 1993). Briefly, hippocampal CA1–CA3 regions were dissected from 1- to 3-day-old Sprague-Dawley rats, dissociated by trypsin treatment followed by trituration with a siliconized Pasteur pipette, and then plated onto coverslips coated with poly-D-lysine (Sigma) inside 6 mm diameter glass cylinder (Bellco Glass) micro-wells. Culture media consisted of minimal essential media (MEM; GIBCO-BRL), 0.6% glucose, 0.1 g/l bovine transferrin (Calbiochem), 0.25 g/l insulin (Sigma), 0.3 g/l glutamine, 5%–10% fetal calf serum (FCS; Sigma), 2% B-27 supplement (GIBCO), and 8 μ M cytosine β -D-arabino-furanoside (Sigma). Cultures were maintained at 37°C in a 95% air, 5% CO₂-humidified incubator, and culture media were replaced every 3–7 days.

Microscopy

Scanning fluorescence and DIC images were acquired using a CLSM designed by Drs. S. J. Smith (Stanford University School of Medicine) and T. A. Ryan (Weill Medical College of Cornell University) using a Zeiss 40 \times 1.3 NA Fluar objective. The system is controlled by software written by one of us (N. E. Z.) and includes provisions for automated, multisite time-lapse microscopy. Cells labeled with FM 4-64 (and EGFP in some experiments) were excited using the 488 nm line of an argon laser. Fluorescence emissions were read using >630 nm long-pass and 500–600 nm band-pass filters, respectively (Chroma). DIC images were acquired by collecting the transmitted laser light with a photomultiplier placed at the end of the Zeiss microscope DIC optical train.

Time-lapse recordings were carried out by averaging two frames collected at each of four focal planes spaced 1 μ m apart. All data were collected at 640 \times 480 resolution, at 12 bits/pixel, with the confocal aperture partially open. To increase experimental throughput, data were collected sequentially from 4–12 predefined sites, using the CLSM robotic XYZ stage to cycle automatically through these sites at predetermined time intervals. Focal drift during the

experiment was corrected automatically using the CLSM's "auto-focus" feature, developed by Dr. S. J. Smith: each time the XYZ stage reached a predefined site, the focal plane of the medium/coverslip interface was determined automatically, and image stacks were collected at predefined offsets above this plane.

Neuronal preparations were mounted in a modified laminar flow chamber (Warner Instrument) and perfused with medium composed of MEM (Biological Industries, Beit Haemek, Israel) supplemented with cytosine β -D-arabino-furanoside (8 μ M), glucose (5 g/l), FCS (5%), DNOX (10 μ M, Research Biochemicals International, Natick, MA), and D,L-AP-5 (50 μ M, RBI). FCS used in experiments was pretreated by dialyzing it for 48 hr at 4°C against 120 mM NaCl to remove cytotoxic amounts of glutamate and aspartate (Schramm et al., 1990). The chamber was placed in a custom designed enclosure flooded with a sterile mixture of 5% CO₂ and 95% air. The chamber, solution inlet, and objective were heated to 37°C–38°C using resistors and thermal foil and were controlled separately. This setup resulted in stable intrachamber temperatures of 34°C–35°C.

Functional Labeling of Presynaptic Boutons with FM 4-64

Functional presynaptic boutons were visualized by loading them with FM 4-64 (N-[3-triethylammoniumpropyl]-4-[6-(4-(diethylamino)phenyl)hexatrienyl]pyridinium dibromide, Molecular Probes). Cells were exposed to FM 4-64 by flooding the perfusion chamber with medium containing 15 μ M FM 4-64. The neurons were then stimulated to fire action potentials by passing 1 ms current pulses through platinum electrodes placed on both sides of the chamber. The cells were stimulated for 30 s at 10 Hz, left in the dye for an additional 30 s, and then rinsed with dye-free medium for 10–15 min.

Expression of Enhanced Green Fluorescent Protein

EGFP transfection of hippocampal neurons (plasmid pEGFP-C1, Clontech) was based on the calcium phosphate transfection method described by Xia et al. (1996), except that the osmotic shock treatment described there was omitted. Briefly, cells raised in culture for 5–7 days were washed with fresh, serum-free medium (MEM + 5 g/l glucose), after saving original media, and left in the incubator for 1 hr. Then, 6 μ l of a calcium phosphate precipitate–DNA mixture was added to each glass cylinder, and cells were returned to the incubator for 30 min. Cells were then washed twice with serum-free medium, after which the original medium was returned to the glass cylinders. Precipitate was prepared by mixing 150 μ l of 2 \times HEPES-buffered solution at pH 7.05 (see Xia et al., 1996) with an equal volume of 0.2 M CaCl₂ to which 10 μ g of plasmid DNA was added. Precipitate mixture was kept at room temperature for 25 min before adding to glass cylinders. Transfection was evaluated after 24 hr by fluorescence microscopy. EGFP was typically expressed in 10–20 neurons/cylinder.

Retrospective Immunohistochemistry

Neurons were fixed by flooding the perfusion chamber with a fixative solution consisting of 4% formaldehyde and 120 mM sucrose in phosphate-buffered saline (PBS) for 20 min, except in experiments in which cells were stained with antibodies against NR1, in which case neurons were fixed with cold (–20°C) methanol for 10 min. The cells were permeabilized for 10 min in fixative solution to which 0.25% Triton X-100 (Sigma) was added. Methanol-fixed cells were also permeabilized with Triton X-100 (0.25% Triton X-100 in PBS). The cells were washed three times in PBS, incubated in 10% bovine serum albumin (BSA) for 1 hr at 37°C, and incubated overnight at 4°C or room temperature with primary antibodies in PBS and 1% BSA. The cells were then rinsed three times for 10 min with PBS and incubated for 1 hr at room temperature with secondary antibodies in PBS and 1% BSA. The cells were rinsed again with PBS, mounted, and imaged immediately.

Primary antibodies used in this study included monoclonal mouse anti-SAP90/PSD-95 (clone 7E3-1B8, Affinity Bioreagents), rabbit polyclonal anti-Bassoon (tom Dieck et al., 1998), mouse monoclonal anti-NR1 (clone 54.1, Pharmingen), and rabbit anti-GluR1 (Chemicon International). Secondary antibodies used were Alexa 488 goat anti-rabbit (Molecular Probes) and Cy5 donkey anti-mouse (Chemicon).

To facilitate finding the location of the sites for which data were

collected during experiments, a small cross was etched on a cell-free region of each coverslip, and coordinates of all sites were stored as offsets from this fiduciary mark to computer files. These coordinate sets were then used to locate the same sites after remounting the fixed and processed specimens on the microscope. Specimen position was then corrected manually by comparing the DIC images obtained during the experiment with those of the fixed tissue, and images of immunolabeled cells were collected by averaging four frames at six sections spaced 0.5 μm apart with the confocal aperture nearly fully closed. Alexa 488 fluorescence was recorded at 488 nm excitation/500–600 nm emission, and Cy5 fluorescence was recorded at 633 nm excitation (Helium-Neon 633 line)/>650 emission.

Data Analysis

All data analysis was performed using software ("OpenView") written for this purpose by one of us (N. E. Z.). Maximal intensity projection images were prepared from all image stacks, and these were used for all subsequent analysis. Digital movies of time-lapse sequences were prepared for each site and thereafter used to detect new FM 4-64-labeled puncta not observed at prior time points. Such puncta were then examined carefully in original image sets, and any bouton for which punctate staining, however faint, was observed in the first image of the time-lapse series was rejected (Figure 1A). Furthermore, for a new punctum to be scored as a new bouton, it had to comply with three additional conditions: (1) it had to be at least 2 μm away from a preexisting bouton, (2) it had to persist until the end of the time-lapse session, and (3) it had to release the dye in response to a train of action potentials.

After new FM 4-64-labeled puncta were marked, their locations were overlaid on corresponding images of the fixed and immunolabeled tissue. To minimize human bias, alignment of FM 4-64 images and retrospective ones was done according to DIC images of the same regions. In some cases, a slight (<2°) relative rotation had to be compensated for. The alignment and rotation settings determined for the DIC images were then used to align the FM 4-64 and immunofluorescent images, and sites at which new FM 4-64-labeled boutons had appeared were examined for the presence or absence of discrete clusters of the immunolabeled protein. If such a cluster was found within 1 μm of the last position of the new FM 4-64-labeled bouton (the position at the moment of fixation), it was scored as a matched bouton. Only clusters with peak fluorescence levels 50% greater than the maximal fluorescence levels of diffuse dendritic staining in the vicinity of the bouton were scored. To minimize errors, regions with large numbers of closely positioned boutons were not analyzed; all analysis was limited to regions in which boutons were well separated from each other. This was not a major problem, however, as synaptic density was usually moderate in the preparations used. After determining the fraction of new boutons matched with immunolabeled clusters, the degree of matching for preexisting boutons was determined in a similar manner.

The "birth date" assigned to an apparently new bouton was dependent on the manner in which it was first observed: for boutons detected after a second or third round of FM 4-64 labeling (as in Figure 1A), the time at which the labeling procedure was performed was considered to be that bouton's "birth date." For boutons observed to form between labeling episodes (as in Figure 1B), the time at which such a cluster was first observed was used.

Due to the strict criteria we used for scoring new boutons, we were left with small numbers of such boutons (about one to two new boutons per site per hour). It was thus pointless to perform a statistical analysis, and the results of each experimental series were aggregated.

Acknowledgments

We are grateful to Larisa Goldfeld and Vladimir Lyakhov for their invaluable technical assistance and to Drs. Shimon Marom, Jackie Schiller and Daniel Dagan for many stimulating discussions. This work was supported by grants from the Israel Science Foundation (139/98) and the National Institute for Psychobiology in Israel (30-99) to N. E. Z. and from the National Institutes of Health (P50

HD32901, AG 12978-02, AG 06569-09) to C. C. G. N. E. Z. is a member of the Bernard Katz Minerva Center for Cell Biophysics.

Received February 1, 2000; revised June 1, 2000.

References

- Ahmari, S.E., Buchanan, J., and Smith, S. J. (2000). Assembly of presynaptic active zones from cytoplasmic transport packets. *Nat. Neurosci.* 3, 445–451.
- Baranes, D., Lederfein, D., Huang, Y.Y., Chen, M., Bailey, C.H., and Kandel, E.R. (1998). Tissue plasminogen activator contributes to the late phase of LTP and to synaptic growth in the hippocampal mossy fiber pathway. *Neuron* 21, 813–825.
- Basarsky, T.A., Parpura, V., and Haydon, P.G. (1994). Hippocampal synaptogenesis in cell culture: developmental time course of synapse formation, calcium influx, and synaptic protein distribution. *J. Neurosci.* 14, 6402–6411.
- Brandstatter, J.H., Fletcher, E.L., Garner, C.C., Gundelfinger, E.D., and Wassle, H. (1999). Differential expression of the presynaptic cytomatrix protein bassoon among ribbon synapses in the mammalian retina. *Eur. J. Neurosci.* 11, 3683–3693.
- Buchanan, J., Sun, Y.A., and Poo, M.M. (1989). Studies of nerve-muscle interactions in *Xenopus* cell culture: fine structure of early functional contacts. *J. Neurosci.* 9, 1540–1554.
- Cho K.O., Hunt, C.A., and Kennedy, M.B. (1992). The rat brain postsynaptic density fraction contains a homolog of the *Drosophila* discs-large tumor suppressor protein. *Neuron* 9, 929–942.
- Cochilla, A.J., Angleson, J.K., and Betz, W.J. (1999). Monitoring secretory membrane with FM1-43 fluorescence. *Annu. Rev. Neurosci.* 22, 1–10.
- Cooper, M.W., and Smith, S. J. (1992). A real time analysis of growth cone-target cell interactions during the formation of stable contacts between hippocampal neurons in culture. *J. Neurobiol.* 23, 814–828.
- Craig, A.M., Blackstone, C.D., Huganir, R.L., and Banker, G. (1993). The distribution of glutamate receptors in cultured rat hippocampal neurons: postsynaptic clustering of AMPA-selective subunits. *Neuron* 10, 1055–1068.
- Craig, A.M., Blackstone, C.D., Huganir, R.L., and Banker, G. (1994). Selective clustering of glutamate and gamma-aminobutyric acid receptors opposite terminals releasing the corresponding neurotransmitters. *Proc. Natl. Acad. Sci. USA* 91, 12373–12377.
- Dai, Z., and Peng, H.B. (1996). Dynamics of synaptic vesicles in cultured spinal cord neurons in relationship to synaptogenesis. *Mol. Cell. Neurosci.* 7, 443–452.
- Dailey, M.E., and Smith, S. J. (1996). The dynamics of dendritic structure in developing hippocampal slices. *J. Neurosci.* 16, 2983–2994.
- Engert, F., and Bonhoeffer, T. (1999). Dendritic spine changes associated with hippocampal long-term synaptic plasticity. *Nature* 399, 66–70.
- Feldman, D.E., and Knudsen, E.I. (1998). Experience-dependent plasticity and the maturation of glutamatergic synapses. *Neuron* 20, 1067–1071.
- Fenster, S.D., Chung, W.J., Zhai, R., Cases-Langhoff, C., Voss, B., Garner, A.M., Kaempf, U., Kindler, S., Gundelfinger, E.D., and Garner, C.C. (2000). Piccolo, a presynaptic zinc finger protein structurally related to Bassoon. *Neuron* 25, 203–214.
- Fletcher, T.L., Cameron, P., De Camilli, P., and Banker, G. (1991). The distribution of synapsin I and synaptophysin in hippocampal neurons developing in culture. *J. Neurosci.* 11, 1617–1626.
- Fletcher, T.L., De Camilli, P., and Banker, G. (1994). Synaptogenesis in hippocampal cultures: evidence indicating that axons and dendrites become competent to form synapses at different stages of neuronal development. *J. Neurosci.* 14, 6695–6706.
- Garner, C.C., Kindler, S., and Gundelfinger, E.M. (2000a). Molecular determinants of presynaptic active zones. *Curr. Opin. Neurobiol.* 10, 321–327.
- Garner, C.C., Nash, J., and Huganir, R.L. (2000b). PDZ proteins in synapse assembly and signaling. *Trends Cell Biol.* 10, 274–280.

- Hall, Z.W., and Sanes, J.R. (1993). Synaptic structure and development: the neuromuscular junction. *Cell* 72 (suppl.), 99–121.
- Henkel, A.W., and Betz, W.J. (1995). Staurosporine blocks evoked release of FM1-43 but not acetylcholine from frog motor nerve terminals. *J. Neurosci.* 15, 8246–8258.
- Hoch, W. (1999). Formation of the neuromuscular junction. Agrin and its unusual receptors. *Eur. J. Biochem.* 265, 1–10.
- Horch, H.W., Kruttgen, A., Portbury, S.D., and Katz, L.C. (1999). Destabilization of cortical dendrites and spines by BDNF. *Neuron* 23, 353–364.
- Jontes, J.D., Buchanan, J., and Smith, S.J. (2000). Growth cone and dendrite dynamics in zebrafish embryos: early events in synaptogenesis imaged *in vivo*. *Nat. Neurosci.* 3, 231–237.
- Kannenbergh, K., Sieghart, W., and Reuter, H. (1999). Clusters of GABA_A receptors on cultured hippocampal cells correlate only partially with functional synapses. *Eur. J. Neurosci.* 11, 1256–1264.
- Kim, J.H., and Huganir, R.L. (1999). Organization and regulation of proteins at synapses. *Curr. Opin. Cell Biol.* 11, 248–254.
- Kistner, U., Wenzel, B.M., Veh, R.W., Cases-Langhoff, C., Garner, A.M., Appeltauer, U., Voss, B., Gundelfinger, E.D., and Garner, C.C. (1993). SAP90, a rat presynaptic protein related to the product of the Drosophila tumor suppressor gene *dlg-A*. *J. Biol. Chem.* 268, 4580–4583.
- Kornau, H.C., Schenker, L.T., Kennedy, M., and Seeburg, P.H. (1995). Domain interaction between NMDA receptor subunits and the postsynaptic density protein PSD-95. *Science* 269, 1737–1740.
- Kossel, A.H., Williams, C.V., Schweizer, M., and Kater, S.B. (1997). Afferent innervation influences the development of dendritic branches and spines via both activity-dependent and non-activity-dependent mechanisms. *J. Neurosci.* 17, 6314–6324.
- Kraszewski, K., Mundigl, O., Daniell, L., Verderio, C., Matteoli, M., and De Camilli, P. (1995). Synaptic vesicle dynamics in living cultured hippocampal neurons visualized with CY3-conjugated antibodies directed against the luminal domain of synaptotagmin. *J. Neurosci.* 15, 4328–4342.
- Lee, S.H., and Sheng, M. (2000). Development of neuron–neuron synapses. *Curr. Opin. Neurobiol.* 10, 125–131.
- Liao, D., Zhang, X., O'Brien, R., Ehlers, M.D., and Huganir, R.L. (1999). Regulation of morphological postsynaptic silent synapses in developing hippocampal neurons. *Nat. Neurosci.* 2, 37–43.
- Ma, L., Zablow, L., Kandel, E.R., and Siegelbaum, S.A. (1999). Cyclic AMP induces functional presynaptic boutons in hippocampal CA3–CA1 neuronal cultures. *Nat. Neurosci.* 2, 24–30.
- Maletic-Savatic, M., Malinow, R., and Suvboda, K. (1999). Rapid dendritic morphogenesis in CA1 hippocampal dendrites induced by synaptic activity. *Science* 283, 1923–1927.
- Mammen, A.L., Huganir, R.L., and O'Brien, R.J. (1997). Redistribution and stabilization of cell surface glutamate receptors during synapse formation. *J. Neurosci.* 17, 7351–7358.
- Matteoli, M., Takei, K., Perin, M.S., Südhof, T.C., and De Camilli, P. (1992). Exo-endocytotic recycling of synaptic vesicles in developing processes of cultured hippocampal neurons. *J. Cell Biol.* 117, 849–861.
- Migaud, M., Charlesworth, P., Dempster, M., Webster, L.C., Watabe, A.M., Makhinson, M., He, Y., Ramsay, M.F., Morris, R.G., Morrison, J.H., et al. (1998). Enhanced long-term potentiation and impaired learning in mice with mutant postsynaptic density-95 protein. *Nature* 396, 433–439.
- Naisbitt, S., Kim, E., Tu, J.C., Xiao, B., Sala, C., Valtschanoff, J., Weinberg, R.J., Worley, P.F., and Sheng, M. (1999). Shank, a novel family of postsynaptic density proteins that binds to the NMDA receptor/PSD-95/GKAP complex and cortactin. *Neuron* 23, 569–582.
- O'Brien, R.J., Mammen, A.L., Blackshaw, S., Ehlers, M.D., Rothstein, J.D., and Huganir, R.L. (1997). The development of excitatory synapses in cultured spinal neurons. *J. Neurosci.* 17, 7339–7350.
- O'Brien, R.J., Kamboj, S., Ehlers, M.D., Rosen, K.R., Fischbach, G.D., and Huganir, R.L. (1998). Activity-dependent modulation of synaptic AMPA receptor accumulation. *Neuron* 21, 1067–1078.
- O'Brien, R.J., Xu, D., Petralia, R.S., Steward, O., Huganir, R.L., and Worley, P. (1999). Synaptic clustering of AMPA receptors by the extracellular immediate-early gene product *Narp*. *Neuron* 23, 309–323.
- Okabe, S., Kim, H.D., Miwa, A., Kuriu, T., and Okado, H. (1999). Continual remodeling of postsynaptic density and its regulation by synaptic activity. *Nat. Neurosci.* 2, 804–811.
- Passafaro, M., Sala, C., Niethammer, M., and Sheng, M. (1999). Microtubule binding by CRIPT and its potential role in the synaptic clustering of PSD-95. *Nat. Neurosci.* 2, 1063–1069.
- Petralia, R.S., Esteban, J.A., Wang, Y.X., Partridge, J.G., Zhao, H.M., Wenthold, R.J., and Malinow, R. (1999). Selective acquisition of AMPA receptors over postnatal development suggests a molecular basis for silent synapses. *Nat. Neurosci.* 2, 31–36.
- Rao, A., and Craig, A.M. (1997). Activity regulates the synaptic localization of the NMDA receptor in hippocampal neurons. *Neuron* 19, 801–812.
- Rao, A., Kim, E., Sheng, M., and Craig, A.M. (1998). Heterogeneity in the molecular composition of excitatory postsynaptic sites during development of hippocampal neurons in culture. *J. Neurosci.* 18, 1217–1229.
- Richter, K., Langnaese, K., Kreutz, M.R., Olias, G., Zhai, R., Scheich, H., Garner, C.C., and Gundelfinger, E.D. (1999). Presynaptic cytomatrix protein bassoon is localized at both excitatory and inhibitory synapses of rat brain. *J. Comp. Neurol.* 408, 437–448.
- Ryan, T.A., and Smith, S. J. (1995). Vesicle pool mobilization during action potential firing at hippocampal synapses. *Neuron* 14, 983–989.
- Ryan, T.A., Reuter, H., Wendland, B., Schweizer, F.E., Tsien, R.W., and Smith, S.J. (1993). The kinetics of synaptic vesicle recycling measured at single presynaptic boutons. *Neuron* 11, 713–724.
- Ryan, T.A., Ziv, N.E., and Smith, S. J. (1996). Potentiation of evoked synaptic turnover at individually resolved synaptic boutons. *Neuron* 17, 125–134.
- Sanes, J.R., and Scheller, R.H. (1997). Synapse formation: a molecular perspective. In *Molecular and Cellular Approaches to Neural Development*, W.M. Cowan et al., eds. (New York: Oxford University Press), pp. 179–219.
- Schramm, M., Eimerl, S., and Costa, E. (1990). Serum and depolarizing agents cause acute neurotoxicity in cultured cerebellar granule cells: role of the glutamate receptor responsive to N-methyl-D-aspartate. *Proc. Natl. Acad. Sci. USA* 87, 1193–1197.
- Serpinskaya, A.S., Feng, G., Sanes, J.R., and Craig, A.M. (1999). Synapse formation by hippocampal neurons from agrin-deficient mice. *Dev. Biol.* 205, 65–78.
- Shapiro, L., and Colman, D.R. (1999). The diversity of cadherins and implications for a synaptic adhesive code in the CNS. *Neuron* 23, 427–430.
- Sheng, M., and Pak, D.T. (1999). Glutamate receptor anchoring proteins and the molecular organization of excitatory synapses. *Ann. NY Acad. Sci.* 868, 483–493.
- Shi, S.H., Hayashi, Y., Petralia, R.S., Zaman, S.H., Wenthold, R.J., Suvboda, K., and Malinow, R. (1999). Rapid spine delivery and redistribution of AMPA receptors after synaptic NMDA receptor activation. *Science* 284, 1811–1816.
- tom Dieck, S., Sanmarti-Vila, L., Langnaese, K., Richter, K., Kindler, S., Soyke, A., Wex, H., Smalla, K.H., Kampf, U., Franzer, J.T., et al. (1998). Bassoon, a novel zinc-finger CAG/glutamine-repeat protein selectively localized at the active zone of presynaptic nerve terminals. *J. Cell Biol.* 142, 499–509.
- Toni, N., Buchs, P.A., Nikonenko, I., Bron, C.R., and Müller, D. (1999). LTP promotes formation of multiple spine synapses between a single axon terminal and a dendrite. *Nature* 402, 421–425.
- Uchida, N., Honjo, Y., Johnson, K.R., Wheelock, M.J., and Takeichi, M. (1996). The catenin/cadherin adhesion system is localized in synaptic junctions bordering transmitter release zones. *J. Cell Biol.* 135, 767–779.
- Verderio, C., Coco, S., Pravettoni, E., Bacci, A., and Matteoli, M.

(1999). Synaptogenesis in hippocampal cultures. *Cell. Mol. Life Sci.* *55*, 1448–1462.

Verhage, M., Maia, A.S., Plomp, J.J., Brussaard, A.B., Heeroma, J.H., Vermeer, H., Toonen, R.F., Hammer, R.E., van den Berg, T.K., Missler, M., et al. (2000). Synaptic assembly of the brain in the absence of neurotransmitter secretion. *Science* *287*, 864–869.

Winter, C., tom Dieck, S., Boeckers, T.M., Bockmann, J., Kampf, U., Sanmarti-Vila, L., Langnaese, K., Altmann, W., Stumm, M., Soyke, A., et al. (1999). The presynaptic cytomatrix protein Bassoon: sequence and chromosomal localization of the human BSN gene. *Genomics* *57*, 389–397.

Xia, Z., Dudek, H., Miranti, C.K., and Greenberg, M.E. (1996). Calcium influx via the NMDA receptor induces immediate early gene transcription by a MAP kinase/ERK-dependent mechanism. *J. Neurosci.* *16*, 5425–5436.

Zhai, R., Olias, G., Chung, W.J., Lester, R.A.J., tom Dieck, S., Langnaese, K., Kreutz, M.R., Kindler, S., Gundelfinger, E.D., and Garner, C.C. (2000). Temporal appearance of the presynaptic cytomatrix protein Bassoon during synaptogenesis. *Mol. Cell. Neurosci.* *15*, 417–428.

Ziv, N.E., and Smith, S. J (1996). Evidence for a role of dendritic filopodia in synaptogenesis and spine formation. *Neuron* *17*, 91–102.